Photosynth Res (2013) 116:93–105
DOI 10.1007/s11120-013-9908-0

REGULAR PAPER

Characterization of photosystem I in rice (*Oryza sativa* L.) seedlings upon exposure to random positioning machine

Boya Chen · Aihong Zhang · Qingtao Lu · Tingyun Kuang · Congming Lu · Xiaogang Wen

Received: 22 April 2013 / Accepted: 30 July 2013 / Published online: 14 August 2013

Abstract To gain a better understanding of how photosynthesis is adapted under altered gravity forces, photosynthetic apparatus and its functioning were investigated in rice (*Oryza sativa* L.) seedlings grown in a random positioning machine (RPM). A decrease in fresh weight and dry weight was observed in rice seedlings grown under RPM condition. No significant changes were found in the chloroplast ultrastructure and total chlorophyll content between the RPM and control samples. Analyses of chlorophyll fluorescence and thermoluminescence demonstrate that PSII activity was unchanged under RPM condition. However, PSI activity decreased significantly under RPM condition. 77 K fluorescence emission spectra show a blue-shift and reduction of PSI fluorescence emission peak in the RPM seedlings. In addition, RPM caused a significant decrease in the amplitude of absorbance changes of P700 at 820 nm (A_{820}) induced by saturated far-red light. Moreover, the PSI efficiency (Φ_I) decreased significantly under RPM condition. Immunoblot and blue native gel analyses further illustrate that accumulation of PSI proteins was greatly decreased in the RPM seedlings. Our results suggest that PSI, but not PSII, is down-regulated under RPM condition.

B. Chen · A. Zhang · Q. Lu · T. Kuang · C. Lu · X. Wen (✉)
Photosynthesis Research Center, Key Laboratory of Photobiology, Institute of Botany, Chinese Academy of Sciences, Beijing 100093, China
e-mail: wenxg@ibcas.ac.cn

B. Chen
University of Chinese Academy of Sciences, Beijing 100049, China

C. Lu
National Center for Plant Gene Research, Beijing 100093, China

Keywords Random positioning machine · Clinorotation · Rice (*Oryza sativa* L.) · Photosynthesis · Photosystem I · Photosystem II

Introduction

Photosynthesis is one of the most important biochemical processes on earth by which the energy of sunlight is converted into chemical forms that support virtually all life on earth. Photosynthesis is also the basis for the use of plants for food production and atmospheric regeneration in the bioregenerative life support system during long-term manned space missions (Eley and Myers 1964; Myers 1954; Salisbury 1991; Wheeler et al. 2001). Plants on earth are subjected to a constant gravitational field. Understanding of the development of photosynthetic apparatus and its functioning under altered gravity forces found in space is crucial for future space exploitation.

Although effects of microgravity on plant growth and development have been extensively studied in the past 50 years, conflicting results were often reported in different spaceflight experiments, especially in the field of photosynthesis and other metabolic processes (Dutcher et al. 1994; Perbal 2006; Wolff et al. 2013; Wolverton and Kiss 2009). Changes in chloroplast morphology and ultrastructure were reported in several spaceflight experiments, including decrease of chloroplast size and grana number per chloroplast, swollen thylakoids, less stroma and grana thylakoid membranes stacking (Adamchuk et al. 2002; Jiao et al. 2004; Kochubey et al. 2004; Nechitailo and Mashinsky 1993; Nedukha 1997). Similar results were obtained in plants grown under simulated microgravity (Adamchuk 1998; Kordyum and Adamchuk 1997). However, few changes in chloroplast ultrastructure were

observed in spaceflight *Arabidopsis* and dwarf wheat grown under well ventilated conditions, suggesting that limited environmental control might be responsible for the significant changes in chloroplast morphology and ultrastructure under spaceflight conditions (Musgrave et al. 1998; Stutte et al. 2006).

In addition to changes in chloroplast development, inhibition of photosynthetic activity was also found in some spaceflight experiments. Reductions in the photosynthetic electron transport rate through photosystem I (PSI), photosystem II (PSII), and the whole chain were observed under saturating light and CO_2 conditions in space-grown dwarf wheat and *Brassica rapa* plants (Stutte et al. 2005; Tripathy et al. 1996; Volovik et al. 1999). The net photosynthetic rate of barley leaves was reduced with decreasing gravity levels from 1.0 to 0.01 g under moderate light during a parabolic airplane flight (Kitaya et al. 2001). Jiao et al. (2004) reported a decrease of PSI electron transport activity in spaceflight *B. rapa* cotyledons, while changes of PSII activity were not studied in their experiment. A decline of excitation energy transfer to PSI was also observed in spaceflight *B. rapa* (Kochubey et al. 2004). So far there is no report of simultaneous studies of photosynthetic apparatus and in vivo PSI and PSII activities under microgravity and clinorotation conditions. It has not been shown whether microgravity affects photochemical activities of both photosystems or only inhibits one of them. A better understanding of the molecular mechanisms of PSI and PSII under microgravity may help to optimize the productivity of plants grown in space.

It should be noted that our knowledge of plant growth and development in space was often based on small samples and lack of proper control groups. In addition, spaceflight experiments were often suffered from insufficient environmental control of plant growth, such as lack of ventilation and ethylene scrubbers in closed chamber, thus leading to compromised experimental results (Monje et al. 2005; Musgrave et al. 1998; Wolverton and Kiss 2009). Under well stirred atmosphere, no significant changes were found in chloroplast ultrastructure and plant stand gas exchange of a spaceflight dwarf wheat cultivar under moderate light illumination and saturating CO_2 concentration (Monje et al. 2005; Stutte et al. 2005, 2006). Until now no consensus has been reached on the response of photosynthesis under microgravity. Due to the short of spaceflight experiments, our knowledge in this field is still limited.

Clinostats can compensate for gravity by continuous change of orientation of objects relative to the gravity's vector. They offer an effective way to mimic certain aspects of the microgravity environment in ground-based research (Hoson et al. 1997; Kraft et al. 2000; Moore 1990). Clinostats also provide opportunities to study the effects of simulated microgravity under sufficient controlled-environment using proper controls and replicates which cannot be easily made under spaceflight conditions. Random positioning machines (RPM), also called 3D clinostats, are recognized to offer a good simulation of microgravity for higher plants. Similarities in the structural polarity, endoplasmic reticulum, and amyloplast position in columella cells were observed under both RPM and true microgravity conditions achieved during spaceflight (Buchen et al. 1993; Hoson et al. 1997; Kraft et al. 2000). RPM has been used in substitution studies to simulate the effects of microgravity on biological processes, such as plant growth, development, and gene expression, in ground-based research (Barjaktarović et al. 2007; Borst and van Loon 2009; Soh et al. 2011; Wei et al. 2010). However, little information of the structure and function of PSI and PSII under RPM condition have been reported.

In this study, we investigated the development of photosynthetic apparatus and its functioning changes of *Oryza sativa* L. plants grown in the RPM and ground control. Our results reveal that exposure to RPM leads to reductions of PSI proteins and photosynthetic activity in the rice seedlings, while PSII proteins and photosynthetic efficiency remain unchanged. Our results suggest that PSI is more susceptible than PSII under RPM condition. The mechanism of photosynthesis under RPM condition is further discussed.

Materials and methods

Plant materials and exposure to RPM

Rice seeds (*Oryza sativa* L. ssp. *japonica* cv. Nipponbare) were planted in the Murashige and Skoog medium containing 1.0 % (w/v) Agar and 3.0 % (v/v) sucrose in the vented-plant culture polycarbonate-bottles.

A two-axis clinostat, also referred as an RPM, was used to simulate effects of microgravity (SM-32, built by Center for Space Science and Applied Research, Chinese Academy of Sciences, China). The RPM consists of two perpendicular and independently driven frames, rotated with randomly varied direction and speed from 1 to −1 rotations min^{-1}, respectively. The sample stage and illumination are settled on the two opposite sides of the inner frame. Details of the RPM were described by Jiang et al. (2008). We modified the illumination by using six extra-bright white light-emitting diodes to increase light intensity. An additional inner frame with the same sample stage and illumination as the RPM was used for the 1 g stationary control experiment. Clinorotation started after the seeds had been planted into the culture medium, and the ground control experiment started at the same time. The

experiments were taken in an air-conditioned room with ambient air and the temperature of 23 ± 1 °C. The light–dark cycle was 12–12 h, and light intensity was 200 μmol m^{-2} s^{-1} at the top of the plants. The control plants grew in the same culture conditions as the plants in the RPM without clinorotation. After growth for 14 days, rice seedlings developed in the RPM and the control were harvested for further experiments. Seedlings developed in the RPM and the control are termed as RPM and CK, respectively.

Transmission electron microscopy (TEM)

For TEM processing, tissues of the youngest fully expanded leaves and root-tips of rice seedlings were cut into small pieces and fixed in 2.5 % (v/v) glutaraldehyde in 0.1 M phosphate buffer (pH 7.2) at 4 °C overnight. Then samples were post fixed in 1 % OsO_4 in the same buffer and washed with 0.1 M phosphate. After that, tissues were dehydrated through a graded ethanol and acetone series and then embedded in Epon-araldite SPURR. After 12 h in pure resin, followed by a change of fresh resin for 4 h, the samples were polymerized at 60 °C for 48 h. Ultrathin sections (70 nm thick) were obtained with a Leica ultramicrotome, stained with uranyl acetate and lead citrate. Electron micrographs were viewed with a transmission electron microscope JEM-1230 TEM (JEOL) at an accelerating voltage of 80 kV.

Chlorophyll (Chl) fluorescence analysis

A PAM-2100 portable fluorometer (Heinz Walz, Germany) was used to measure pulse amplitude-modulated Chl fluorescence, as described by Zhang et al. (2011). Leaves were dark-adapted at room temperature (23 °C) for 30 min. After that, F_o (minimum Chl fluorescence of dark-adapted state) was measured by a weak red light. F_m (maximum Chl fluorescence of dark-adapted state) was determined during a subsequent saturating pulse of white light (8,000 μmol m^{-2} s^{-1} for 0.8 s). Then actinic light at an intensity of 200 μmol m^{-2} s^{-1} (which is equivalent of growth light intensity) was applied continuously for about 7 min. F_s (steady-state Chl fluorescence) was thereafter recorded and a second saturating pulse of white light (8,000 μmol m^{-2} s^{-1} for 0.8 s) was applied to determine F_m' (maximum Chl fluorescence level in the light-adapted state). Then, the actinic light was removed and F_o' (minimal Chl fluorescence level in the light-adapted state) was recorded by applying a 3 s pulse of far-red light. Using the above fluorescence parameters, we calculated: (1) the maximal efficiency of PSII photochemistry in the dark-adapted state, $F_v/F_m = (F_m - F_o)/F_m$; (2) the actual PSII efficiency, $\Phi_{PSII} = (F_m' - F_s)/F_m'$; (3) the photochemical quenching coefficient, $qP = (F_m' - F_s)/(F_m' - F_o')$; (4) the non-photochemical quenching, $NPQ = F_m/F_m' - 1$.

Measurements of the polyphasic Chl fluorescence transients (OJIP) and the analysis of the JIP-test

The polyphasic Chl fluorescence transients were measured by using a Plant Efficiency Analyzer (PEA, Hansatech Instruments Ltd., King's Lynn, Norfolk, UK), according to Strasser et al. (1995). The transients were induced by red light of about 3,000 μmol m^{-2} s^{-1} provided by an array of six light-emitting diodes (peak 650 nm), which focused on the sample surface to give homogenous illumination over the exposed area of the sample (4 mm in diameter). The fluorescence signals were recorded within a time scan from 10 μs to 1 s with a data-acquisition rate of 10,000 points per second for the first 2 ms and of 1,000 points per second after 2 ms. Chl fluorescence transients were analyzed according to the JIP test (Krüger et al. 1997; Strasser and Strasser 1995). All samples were dark-adapted at room temperature (23 °C) for 30 min prior to the measurements.

Thermoluminescence (TL) measurements

Thermoluminescence (TL) measurements were performed with the thermoluminescence extension of the Double-Modulated Fluorometer FL2000-S/F, consisting of Thermoregulator TR2000 (Photon Systems Instruments, Brno, Czech Republic). According to Zhang et al. (2011), after 30-min dark-adaptation, the samples were cooled to −5 °C and illuminated with a single-turnover flash. Then the samples were warmed up to 50 °C at a heating rate of 0.5 °C s^{-1} and the TL light emission was measured during the heating. For $S_2Q_A^-$ recombination studies, leaves were measured in the presence of 50 μM dichlorophenyldimethylurea (DCMU) after the flash illumination.

Oxidation–reduction kinetics of P700 measurements

The light-induced redox kinetics of P700 were monitored by measuring absorbance changes at 820 nm (A_{820}) using a PAM-101 fluorometer connected to an emitter-detector unit ED 800T (Heinz Walz), as described by Meurer et al. (1996). P700 was oxidized by a pulse of red activate light (650 nm, 2,000 μmol m^{-2} s^{-1}, 200 ms duration). Absorbance changes induced by saturated far-red light were used to estimate the photochemical capacity of PSI.

Efficiency of energy conversion in PSI was measured at room temperature with a dual-wavelength pulse-amplitude modulated P700 and fluorescence monitoring system (Dual-PAM-100, Heinz Walz, Effeltrich, Germany), according to Klughammer and Schreiber (2008), Pfündel et al. (2008), and the manufacturer's instructions. Samples

were dark-adapted for 30 min prior to the measurements. P700 was measured via its absorbance change in the near-infrared (transmission or remission difference signal 875–830 nm). After 830 and 875 nm signals were balanced, the zero P700 signal level P_o for fully reduced P700 is determined. P_m, the maximum P700 signal observed upon full oxidation, was measured by a saturating pulse of white light (8,000 μmol m^{-2} s^{-1} for 0.8 s) after 10 s FR preillumination. Then actinic light at an intensity of 200 μmol m^{-2} s^{-1} (which is equivalent of growth light intensity) was applied continuously for about 6 min. P (P700 signal) was thereafter recorded and a second saturating pulse of white light (8,000 μmol m^{-2} s^{-1} for 0.8 s) was applied to determine P_m' (maximum P700 signal in the light-adapted state). Using the above parameters, we calculated: (1) the effective photochemical quantum yield of PSI, $\Phi_I = (P_m' - P)/P_m$; (2) the quantum yield of non-photochemical energy dissipation due to donor side limitation of PSI, $\Phi_{ND} = (P - P_o)/P_m$; (3) the quantum yield of non-photochemical energy dissipation due to acceptor side limitation of PSI, $\Phi_{NA} = (P_m - P_m')/P_m$.

Low-temperature Chl fluorescence emission spectra measurements

Low temperature (77 K) Chl fluorescence emission spectra of thylakoid membranes (5 μg chl mL^{-1}) were recorded with a fluorescence spectrophotometer (Hitachi F-7000). The excitation wavelength was 436 nm (slit 5 nm) and the emission was between 650 and 780 nm (slit 2.5 nm).

BN-PAGE, SDS-PAGE, and immunoblot analysis

BN-PAGE was performed as described by Peng et al. (2006). The thylakoid membranes were washed in 330 mM sorbitol and 50 mM BisTris–HCl, pH 7.0, and suspended in resuspension buffer (20 % glycerol and 25 mM BisTris–HCl, pH 7.0) at 1.0 mg Chl mL^{-1}. An equal volume of resuspension buffer containing 4 % (w/v) DM was added to the thylakoid suspension in a dropwise manner. After incubation at 4 °C for 5 min, insoluble material was removed by centrifugation at 12,000*g* for 10 min. The supernatant was combined with one-tenth volume of 5 % Serva blue G in 100 mM BisTris–HCl, pH 7.0, 0.5 M 6-amino-*n*-caproic acid, and 30 % (w/v) glycerol, and applied to 0.75-mm-thick 5–12 % acrylamide gradient gels in a Hoefer Mighty Small vertical electrophoresis unit connected to a cooling circulator. For two-dimensional SDS-PAGE analysis, excised BN-PAGE lanes were soaked in SDS sample buffer and 5 % β-mercaptoethanol for 30 min and layered onto 1-mm-thick 16 % SDS polyacrylamide gels containing 6 M urea (Laemmli 1970).

Protein extracts for immunoblot analysis were prepared as described (Martínez-Garcia et al. 1999). For immunoblot analysis, total leaf proteins were separated using 15 % SDS polyacrylamide gels containing 6 M urea (Laemmli 1970). After electrophoresis, proteins were transferred electrophoretically to polyvinylidene difluoride membrane (Amersham Biosciences, USA), probed with specific primary antibodies, and visualized by the enhanced chemiluminescence method. X-ray films were scanned and analyzed by using ImageMaster™ 2D Platinum software. The PsaA, PsaB, and Lhca1-4 antibodies were purchased from Agrisera. All the other antibodies were produced in our laboratory according to Peng et al. (2006).

Measurements of Chl and protein contents

Chl content was determined according to Arnon (1949). Protein content was determined by the method of Bradford (1976).

Results

Starch grains distribution in the columella cells of rice seedlings developed in the RPM

Previous studies have shown that starch grains are scattered in the root-cap columella cells under microgravity conditions instead of localized mostly to the distal part of the cell under normal 1 g force field of earth (Buchen et al. 1993; Hoson et al. 1997; Kraft et al. 2000). Our results show that starch grains had a scattered distribution in the columella cells of rice seedlings developed in the RPM, suggesting that RPM can mimic the effects of weightlessness (Fig. 1).

Growth and Chl content of rice seedlings developed in the RPM

The 14-day-old rice seedlings developed in the RPM were disoriented, while the control seedlings exhibited oriented growth relative to gravity. Table 1 shows the growth parameters and Chl content in rice seedlings developed in the RPM and the control. No significant differences were observed in the root-length, shoot-length, and the ratio of root/shoot between the RPM and the control groups, while the shoot-width decreased by 8.7 % in the RPM seedlings. Fresh weight (FW) and dry weight (DW) per seedling significantly decreased by 16.3 and 19.5 %, respectively, indicating reduction of the accumulation of biomass under clinorotation. Total Chl content decreased slightly in the RPM samples, without statistical significance.

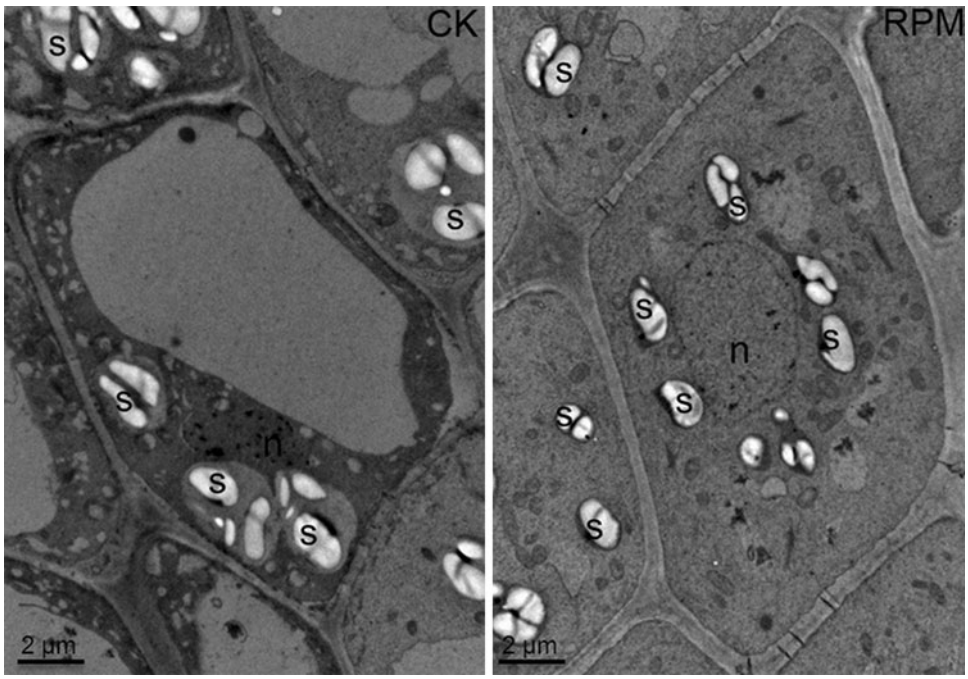

Fig. 1 Electron micrographs of columella cells of rice seedlings developed in the RPM and the CK. *n* nucleus, *s* starch, *bar* 2 μm

Table 1 Growth parameters and Chl content of 14-day-old rice seedlings developed in the RPM and the CK

	CK	RPM
Shoot-length (cm plant^{-1})	19.29 ± 1.18	18.49 ± 0.87
Shoot-width (mm plant^{-1})	2.86 ± 0.26*	2.61 ± 0.35*
Root-length (cm plant^{-1})	6.50 ± 0.55	6.62 ± 0.74
Root/shoot	0.34 ± 0.03	0.36 ± 0.04
FW (mg plant^{-1})	161 ± 18*	135 ± 23*
DW (mg plant^{-1})	21.28 ± 2.63*	17.12 ± 2.01*
Chl (mg g^{-1} FW)	4.36 ± 0.41	4.03 ± 0.46
Chl a/b	2.88 ± 0.33	2.95 ± 0.28

Mean values ± SD of shoot-length, shoot-width, root-length, and the ratio of root/shoot were calculated from 30 seedlings of three independent experiments. Mean values ± SD of FW (Fresh weight), DW (Dry Weight), total Chl content, and the ratio of Chl a/b were calculated from three independent experiments, each taken from a population of 20 seedlings

* $p < 0.05$

Chloroplast ultrastructure of rice seedlings developed in the RPM

Figure 2 shows the electron micrographs of mesophyll chloroplasts and thylakoid membranes of the RPM and the control samples. The chloroplasts of the RPM samples kept their normal shapes compared to the control samples, with thylakoid membranes arranged into compacted grana stacks and a limited number of stroma lamella. No significant differences were found in the length of chloroplast, the number of grana per chloroplast, the number of grana lamella per granum, and the width and length of grana lamella between the RPM and the control samples. Only the width of the chloroplast was significantly decreased in the RPM seedlings (Table 2).

No change in PSII activity was observed in rice seedlings grown in the RPM

Photosynthetic activity is one of the major factors limiting plant biomass accumulation. The decrease of DW observed under RPM condition suggested that the functions of PSII and PSI might be affected. To characterize the PSII photochemical activity and electron transport under clinorotation, pulse amplitude-modulated fluorescence induction, and OJIP transient of the youngest fully expanded leaves of rice seedlings developed in the RPM and the control were investigated. The maximal efficiency of PSII photochemistry, F_v/F_m, was 0.82 and 0.81, respectively, in the RPM and the control samples (Table 3). No significant changes were detected in the actual PSII efficiency (Φ_{PSII}), the photochemical quenching coefficient (qP), and the non-photochemical quenching (NPQ) between the two groups. In addition, no significant changes were found in the parameters related to the electron transport and energy flux of PSII derived from the OJIP transients of the RPM and the control samples. The probability of electron transfer beyond Q_A (Ψ_0), the yield of electron transport beyond Q_A^- (φE_0), absorption flux per reaction center (RC) (ABS/RC), trapped energy flux per RC (TR_0/RC), electron transport flux per RC (ET_0/RC) and dissipated energy flux per RC (DI_0/RC) remained unchanged in rice seedlings grown in the RPM (Table 3).

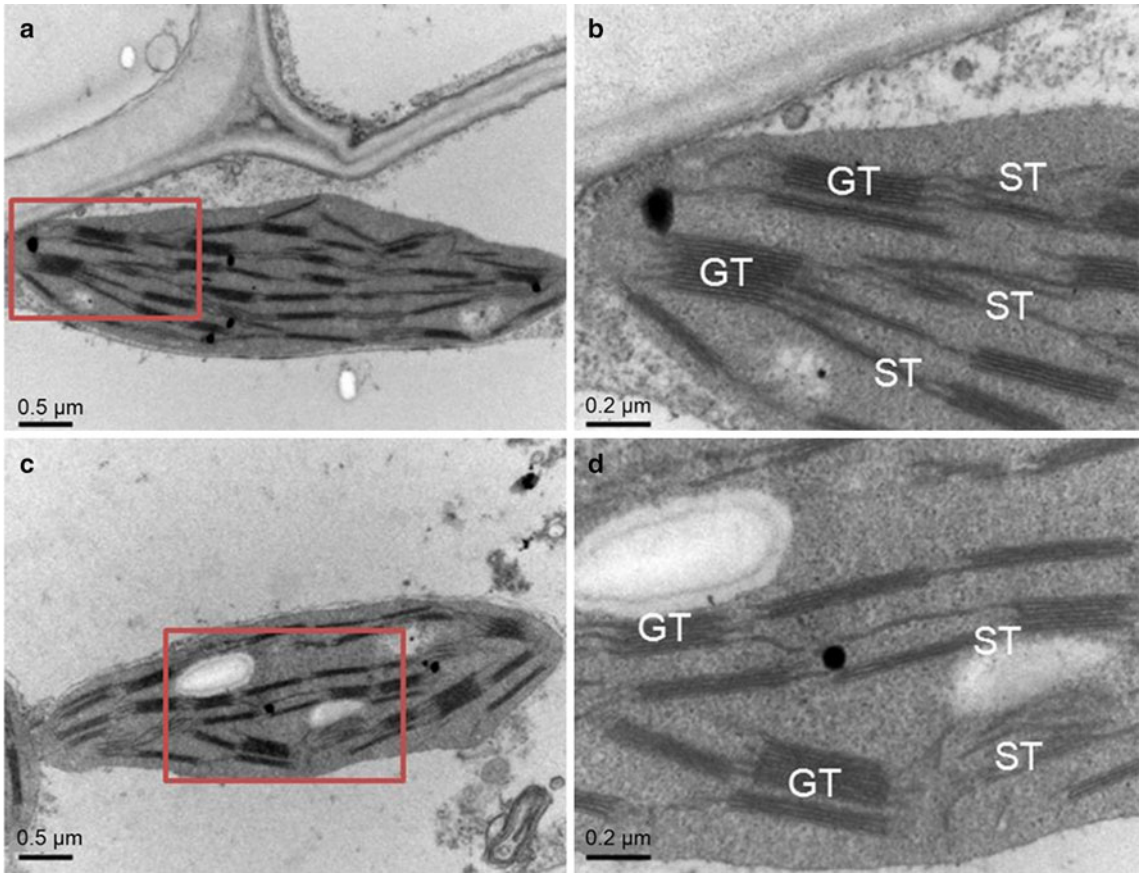

Fig. 2 Electron micrographs of mesophyll chloroplast and thylakoid membranes from rice seedlings developed in the RPM and the control. To quantify the differences between chloroplasts of the RPM and the control samples, 26 chloroplast sections of each sample were analyzed from the youngest fully expanded leaves. **a**, **b** are from the control samples; **c**, **d** are from the RPM samples. **a**, **c** are chloroplasts; **b**, **d** are thylakoid membranes. *GT* grana thylakoids, *ST* stroma thylakoids. *Bars* 0.5 μm in **a** and **c**, and 0.2 μm in **b** and **d**

Table 2 Fluorescence parameters of rice seedlings developed in the RPM and the CK

	CK	RPM
F_v/F_m	0.82 ± 0.01	0.81 ± 0.01
Φ_{PSII}	0.67 ± 0.01	0.66 ± 0.01
qP	0.85 ± 0.03	0.84 ± 0.02
NPQ	0.22 ± 0.02	0.23 ± 0.04
V_J	0.54 ± 0.05	0.51 ± 0.02
V_I	0.85 ± 0.03	0.83 ± 0.02
Ψ_0	0.48 ± 0.02	0.49 ± 0.02
φE_0	0.39 ± 0.02	0.40 ± 0.02
ABS/RC	3.80 ± 0.23	3.80 ± 0.21
TR_0/RC	3.09 ± 0.17	3.14 ± 0.13
DI_0/RC	0.70 ± 0.08	0.65 ± 0.06
ET_0/RC	1.48 ± 0.07	1.53 ± 0.05

Mean ± SD values were calculated from four to six independent experiments

Table 3 Absorbance changes at 820 nm (ΔA_{820}) of rice seedlings developed in the RPM and the CK

	CK	RPM
ΔA_{820}	1.000 ± 0.163*	0.625 ± 0.070*
Φ_I	0.846 ± 0.006*	0.736 ± 0.050*
Φ_{ND}	0.051 ± 0.013	0.059 ± 0.022
Φ_{NA}	0.103 ± 0.011*	0.205 ± 0.052*

Mean ± SD values were calculated from five independent experiments. ΔA_{820} were relative values normalized to the control

* $p < 0.05$

Since TL is a useful tool to study charge stabilization and subsequent recombination in PSII, it was further used to investigate the redox properties of the acceptor and donor sides of PSII in the RPM and the control plants. Recombination of positive charges stored in the S_2 and S_3 oxidation states of the water-oxidizing complex with electrons stabilized on the reduced Q_A and Q_B acceptors of PSII results in characteristic TL emissions (Ducruet and Vass 2009; Inoue 1996). The TL intensity is indicative of the amount of recombining charges, whereas the peak temperature reflects the energetic stabilization of the separated charge pair (Vass et al. 1981). Illumination of a single-turnover flash to the dark-adapted plants induces a

major TL band called the B-band, which appears at 30–38 °C and arises from $S_2/S_3Q_B^-$ recombination. If electron transfer between Q_A and Q_B is blocked by DCMU, the B-band is replaced by the so-called Q-band arising from $S_2Q_A^-$ recombination at 0–10 °C (Demeter and Vass 1984; Ducruet and Vass 2009; Rutherford et al. 1982).

We thus investigated the effects of RPM on the TL glow curves in plants developed in the RPM and the control. There were no significant differences between the RPM and control plants in the peak temperatures and peak intensities of TL glow curves in the absence (Fig. 3a) or presence (Fig. 3b) of DCMU. Both plants exhibited TL emission maxima for the $S_2/S_3Q_B^-$ and $S_2Q_A^-$ charge recombination at ~30 and 1 °C, respectively, demonstrating that clinorotation did not affect the charge stabilization and recombination of PSII.

The above results of Chl fluorescence and TL curves suggest that PSII function is not affected under RPM condition.

PSI activity was reduced in rice seedlings grown in the RPM

In order to investigate the effects of clinorotation on excitation energy transfer between PSII and PSI, changes in the 77 K Chl fluorescence emission spectra of thylakoid membranes of rice seedlings grown in the RPM and the control were further studied (Fig. 4). The fluorescence emission spectra were obtained with excitation at 436 nm, which was absorbed mainly by Chl *a*. There are two main bands with the maximum peaks at about 685 and 735–740 nm, originated from PSII and PSI, respectively (Govindjee 1995; Krause and Weis 1991). The PSII emission band originates mainly from the PSII core complex and the light harvesting complex of PSII (LHCII), while the PSI band originates from the PSI core complex and the light harvesting complex of PSI (LHCI) (Govindjee 1995; Murata and Satoh 1986; Tang et al. 2005).

Both the RPM and control thylakoids exhibited the emission maxima at 685 nm, characteristic for a functional PSII. To clearly show the excitation energy transfer between PSII and PSI, the 77 K fluorescence spectra were normalized to the PSII emission maximum at 685 nm. Clinorotation induced an 11.1 % decrease of maximum fluorescence emission band of PSI compared to the control, suggesting that excitation energy tended to transfer to PSII rather than to PSI (Fig. 4). In addition, the PSI peak at 738 nm in the control thylakoids was shifted to 734 nm in the RPM thylakoids. The blue-shift and reduction of PSI fluorescence emission peak indicate a reduction of energy transfer in PSI and a possible decrease of functional PSI proteins under clinorotation.

We further investigated the redox kinetics of P700 by measuring absorbance changes at 820 nm (A_{820}), representing the photochemical activity of PSI (Klughammer and Schreiber 1994, 1998). The amplitudes of changes in A_{820} induced by saturated far-red light were reduced by 37.5 % in rice seedlings grown in the RPM compared to the control plants, demonstrating a reduction of PSI activity (Fig. 5; Table 4). PSI photochemical efficiency was studied by the P700 slow induction kinetic curves. In the light-adapted state, the effective photochemical quantum yield of PSI (Φ_I) of the control and RPM seedlings were 0.846 and 0.736, respectively, with a significant reduction in the RPM by 13.0 % (Table 4). The quantum yield of non-photochemical energy dissipation due to acceptor side limitation of PSI (Φ_{NA}) of the control and RPM seedlings were 0.103 and 0.205, respectively. Thus, the reduction of Φ_I of the RPM seedlings was mainly due to the increase of Φ_{NA}. The results of 77 K fluorescence emission and redox kinetics of P700 suggest that both PSI proteins and function were inhibited under RPM condition.

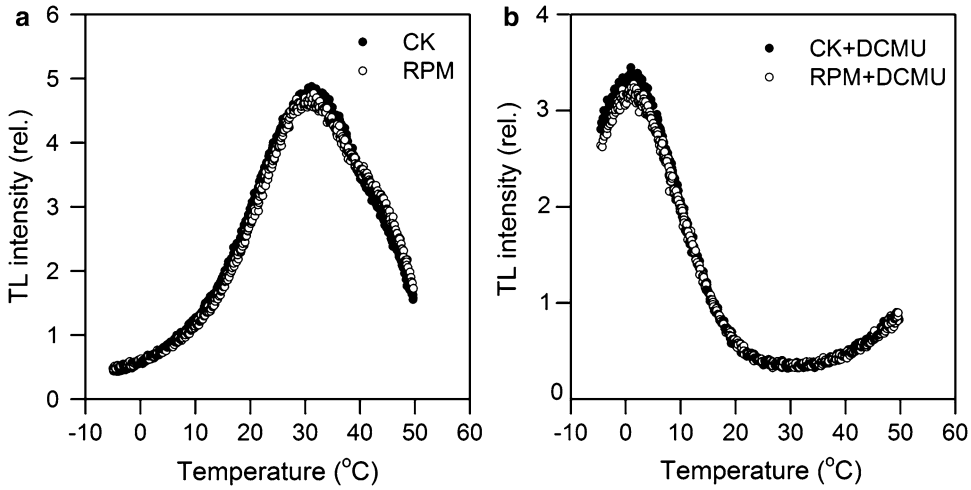

Fig. 3 Thermoluminescence glow curves of rice seedlings developed in the RPM and the CK. The leaves were excited with a single flash in the absence of DCMU (**a**) and in the presence of 50 μM DCMU (**b**). Each *curve* was the mean value of five independent experiments measured of the youngest fully expanded leaves

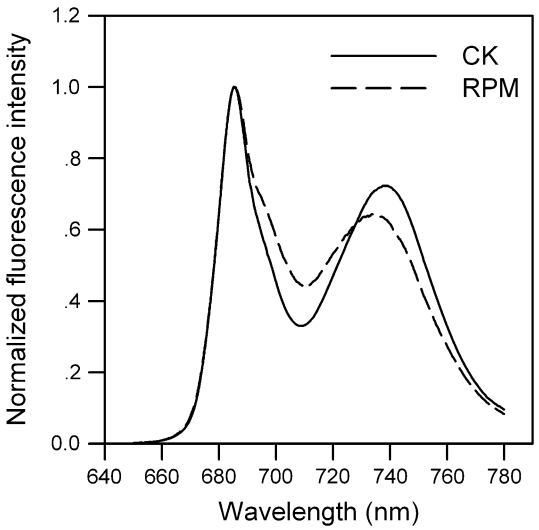

Fig. 4 77 K fluorescence emission spectra of thylakoid membranes of rice leaves developed in the RPM and the CK after excitation at 436 nm. The fluorescence emission signals were normalized to the PSII emission maximum at 685 nm. Each *curve* was the mean value of five independent experiments

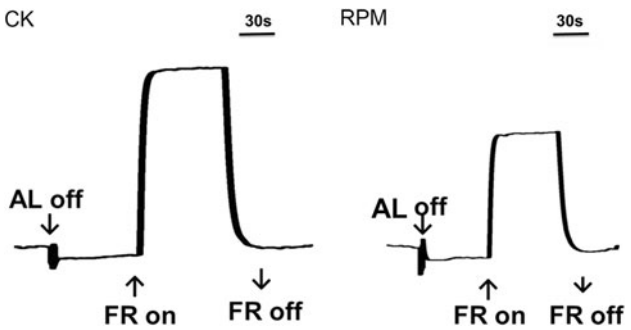

Fig. 5 P700 redox kinetics of rice seedlings developed in the RPM and the CK. The redox kinetics were investigated by measuring absorbance changes of P700 at 820 nm induced by far-red light (FR, 720 nm). *AL* actinic light (650 nm, 2,000 μmol m^{-2} s^{-1}, 200 ms duration). Five independent biological replicates were performed and a representative one is shown

Contents of PSI proteins decreased in rice seedlings grown in the RPM

We further investigated the effects of RPM on the contents of thylakoid membrane proteins by the method of immunoblot (Fig. 6a). As we know, the thylakoid membranes harbor four multiprotein complexes: PSI, PSII, cytochrome b_6f complex (Cyt b_6f), and ATP synthase, which catalyzed the light-reactions of oxygenic photosynthesis in higher plants and cyanobacteria. No significant differences were observed in the contents of PSII proteins (D1, D2, CP43, CP47, LHCII, and PsbO) between the RPM and the control plants, whereas the amount of PSI subunits significantly decreased in the RPM seedlings. In the RPM plants, PsaA and PsaB, the reaction center proteins of PSI, decreased to 77 and 74 % of those in the control plants. The levels of PSI antenna proteins Lhca1, Lhca2, Lhca3, and Lhca4 in the RPM plants were about 70–89 % of those in the control plants. There was no significant change in the amount of large subunit of Rubisco (RbcL) in the RPM plants, while the amount of $CF_1\beta$ protein, β chain of ATP synthase, was reduced to about 79 % of the control plants. Cyt f, subunit of Cyt b_6f which participated in electron transfer between PSII and PSI and NdhH, subunit of NADH dehydrogenase complex (NDH) which mediates PSI cyclic electron transport, slightly decreased by 9 and 8 %, respectively, in the RPM plants.

Table 4 Parameters of chloroplast development in the 14-day-old rice seedlings developed in the RPM and the CK

	CK	RPM
Length of chloroplast (μm)	5.30 ± 0.49	5.29 ± 0.65
Width of chloroplast (μm)	2.58 ± 0.25**	2.27 ± 0.31**
Number of grana per chloroplast	38.13 ± 6.66	37.71 ± 5.67
Number of grana lamella per granum	8.25 ± 2.48	7.37 ± 2.32
Width of grana lamella (nm)	105.48 ± 35.04	104.43 ± 38.74
Length of grana lamella (nm)	393.55 ± 61.57	392.37 ± 48.37

Values in the table are mean ± SE from three independent experiments. To quantify the differences between chloroplasts of the RPM and the control samples, 33 chloroplast sections of each sample were analyzed from the youngest fully expanded leaves

** $p < 0.01$

To further investigate the possible changes in the structure of thylakoid proteins, chlorophyll–protein complexes were solubilized from thylakoid membranes using dodecyl-β-D-maltopyranoside (DM) and separated by BN-PAGE and subsequent SDS-PAGE. In the first dimension, the native thylakoid membrane complexes were separated into six major bands, representing PSII supercomplexes (band I), PSI, LHCI, and dimeric PSII (band II), PSI (band III), monomeric PSII, CP43-free PSII, ATPase, and Cyt b_6f (band IV), trimeric LHCII (band V), and monomeric LHCII (band VI), according to Chen et al. (2007) and Peng et al. (2006) (Fig. 6b). The BN-PAGE analysis showed that the amount of PSI per unit of chlorophyll (band III) decreased in the RPM plants (Fig. 6b). Analyses of the SDS-PAGE gels followed by the BN-PAGE further confirmed that there were significant decreases in the amounts of the PSI proteins in the seedlings developed in the RPM, whereas no PSII proteins were reduced under clinorotation. The amounts of PSI core subunits PsaA/B, two minor subunits of PSI core and Rieske Fe–S protein (Pet C), subunit of Cyt b_6f, were markedly reduced in the RPM plants (Fig. 6c). No significant differences in the amounts

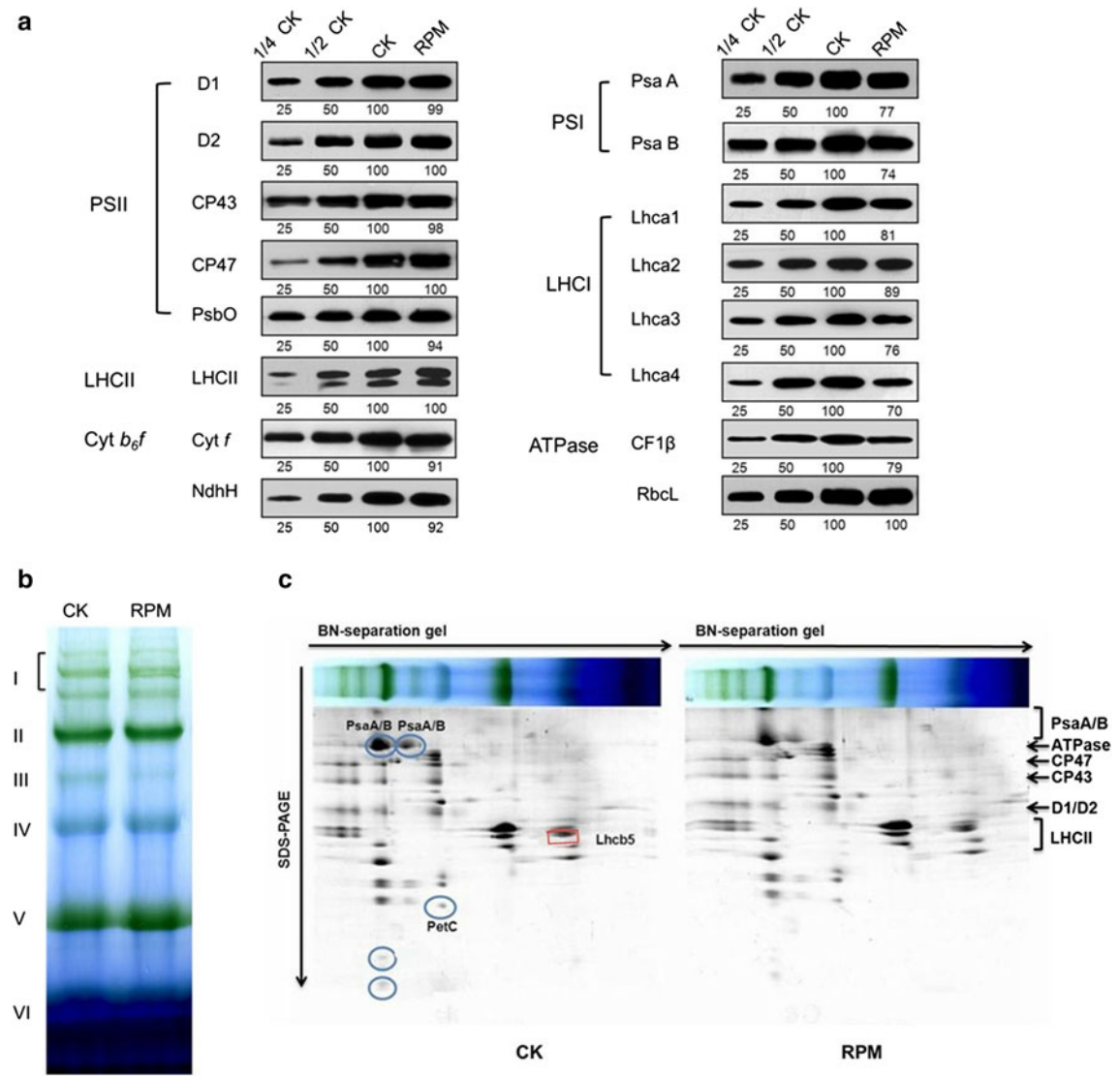

Fig. 6 Analyses of thylakoid membrane proteins from rice seedlings developed in the RPM and the CK. **a** Immunoblot analysis of thylakoid membrane proteins loaded on the basis of equal total leaf proteins (15 mg). Designations of thylakoid membrane protein complexes and their diagnostic components are labeled at *left*. The percentage protein levels shown *below the lanes* were estimated by comparison with levels of corresponding thylakoid proteins of CK. **b** BN gel analysis of thylakoid membrane protein complexes (10 μg chlorophyll). **c** 2D BN/SDS-PAGE fractionation of thylakoid membrane protein complexes. The differential identical proteins are marked by *rectangle* (up-regulated) and *circle* (down-regulated), respectively, with the identity of relevant proteins indicated nearby. For each experiment, three independent biological replicates were performed and a representative one is shown

of the PSII subunits were observed between the RPM and the control plants, except that Lhcb5 increased in the RPM (Fig. 6c). The above results are consistent with the decrease of PSI activity and the maintenance of PSII activity under RPM condition.

Discussion

Although some previous studies have been focused on changes in photosynthetic processes under microgravity, it is still controversial how photosynthesis is adapted to altered gravity forces. Microgravity has been reported to influence the structure and function of photosynthetic apparatus. Altered chloroplast morphology and ultrastructure, decreased levels of photosynthetic pigments, proteins, and activities were observed under both microgravity and simulated microgravity conditions (Adamchuk 1998; Jiao et al. 2004; Kitaya et al. 2001; Kochubey et al. 2004; Stutte et al. 2005; Tripathy et al. 1996). However, recent spaceflight experiments suggested that insufficient environmental control of the plant-growing facilities, such as limited free convection under microgravity, ethylene accumulation, high humidity, and fluctuating temperature levels in

closed chamber, together with lack of proper ground controls sometimes were responsible for the negative effects of photosynthesis under microgravity conditions (Monje et al. 2005; Stutte et al. 2006). Net canopy photosynthesis measured directly under microgravity of a dwarf wheat cultivar grown in a well-controlled plant growth facility was not altered under moderate light illumination and saturating CO_2 concentration (Stutte et al. 2005; Monje et al. 2005). On the other hand, postflight studies in the same experiment also demonstrated reductions of the electron transport rate of PSI, PSII, and the whole chain under saturating light intensity, similar to some previous studies (Stutte et al. 2005). It should be noted that canopy photosynthesis is dependent on the photosynthetic rate per unit leaf area, canopy architecture, light interception, and photosynthetic duration (Long et al. 2006; Parry et al. 2011). Changes in the canopy architecture and light interception under microgravity may compensate for the decrease of photosynthetic rate, thus maintain the net canopy photosynthesis rate and the amount of carbon accumulation. Since only a few spaceflight experiments using limited plant species have attempted to study the effect of altered gravity forces on photosynthesis, the molecular mechanisms of photosynthesis response to microgravity is still far from clear. In this work, we investigated changes of the chloroplast ultrastructure, PSII and PSI photosynthetic activity, and photosynthetic membrane proteins upon exposure to RPM, which simulates certain aspects of microgravity by continuous change of orientation of objects relative to the gravity's vector. To the best of our knowledge, this is the first report using noninvasive in vivo spectroscopy measurements and biochemical analyses to investigate the molecular mechanisms of PSI and PSII upon exposure to RPM. The environmental conditions were carefully controlled and the ground control experiments were properly achieved. The vented plant culture bottles used in our experiments provided sufficient air exchange with the ambient environment to avoid ethylene accumulation and high humidity.

The rice seedlings developed in the RPM were disoriented, with scattered distribution of starch grains in columella cells of root-cap (Fig. 1). The morphology of seedlings and starch grains position in root-cap columella cells were similar to the results of the spaceflight studies, demonstrating that RPM provides an effective way to simulate effects of microgravity in ground research (Buchen et al. 1993; Hoson et al. 1997; Kraft et al. 2000).

Some early reports described disruption of the membrane apparatus for photosynthesis under microgravity and clinorotation conditions, such as decrease of chloroplast size and grana number per chloroplast, less grana lamella stacking, increase in partial volumes of stroma lamella, and swelling of grana (Adamchuk 1998; Jiao et al. 2004; Kochubey et al. 2004; Kordyum and Adamchuk 1997; Nedukha 1997). However, recent spaceflight experiments demonstrated that chloroplasts ultrastructure can be unaffected by exposure to microgravity when air-flow was provided in plant chambers, suggesting that limited environmental control might be responsible for the significant changes in leaf ultrastructure (Musgrave et al. 1998; Stutte et al. 2006). In this work, we demonstrated little difference in the ultrastructure of thylakoid membranes of rice seedlings developed in the RPM under well-controlled environmental conditions (Fig. 2). No differences in the length of chloroplast, the number of grana per chloroplast, the number of grana lamella per granum, the width and length of grana lamella were observed between the RPM and the control, only the average width of the chloroplasts was decreased in the RPM seedlings (Table 2).

However, a decrease of biomass accumulation under RPM condition was observed in our work. DW, FW, and shoot-width per seedling significantly decreased in the RPM sample, while no differences in the shoot-length, root-length, and Chl content were found between the RPM and the control seedlings (Table 1).

To identify the correlation between the reduction of biomass accumulation and photosynthetic efficiency, we further investigated the photosynthetic activities of PSII by noninvasive fluorescence induction kinetics, TL curves, and biochemical analyses. No change of PSII activities was found under RPM condition (Table 3). Only a slight decrease in F_v/F_m was observed in the RPM seedlings compared to the control, suggesting no change in the PSII primary charge separation (Krause and Weis 1991). There were no significant changes in Φ_{PSII} and the derived parameters of electron transport and energy flux from the OJIP curves between the RPM and control seedlings (Table 3). In addition, no significant differences were observed in the peak temperatures and peak intensities of B-band and Q-band of TL glow curves between the rice seedlings developed in the RPM and the control, suggesting the charge stabilization and recombination of the PSII electron acceptors Q_A^- and Q_B^- with the S_2/S_3 oxidation states of the water-oxidizing complex were not affected under RPM condition (Demeter and Vass 1984; Rutherford et al. 1982; Vass et al. 1981) (Fig. 3).

Chlorophyll-binding proteins play an important role in photosynthetic function, but only a few works have been done concerning changes of thylakoid membranes proteins under microgravity and clinorotation conditions. Jiao et al. (2004) reported decreases of both PSI and PSII proteins in spaceflight *B. rapa* plants. Immunoblot analyses in our study showed that the levels of the PSII proteins D1, D2, CP43, CP47, PsbO, and LHCII were unchanged in seedlings developed in the RPM (Fig. 6a). Only one increased PSII protein, Lhcb5, was identified in the RPM seedlings in

the SDS-PAGE gels followed by the BN-PAGE (Fig. 6c). Together with the slight changes in F_v/F_m, Φ_{PSII}, and TL glow curves, we concluded that PSII was well functioned under RPM condition.

On the other hand, our data on 77 K fluorescence emission spectra, redox kinetics of P700, and thylakoid membrane proteins analyses suggested that the photosynthetic activity of PSI significantly decreased in rice seedlings developed in the RPM. The maximum amplitude of absorbance changes of P700 at 820 nm (A_{820}) in the RPM reduced by 37.5 % of the control (Fig. 5; Table 4), demonstrating a reduction of PSI activity under RPM condition (Chen et al. 2007; Meurer et al. 1996). In addition, Φ_I of the RPM seedlings significantly reduced by 13.0 % compared to the control seedlings (Table 4). The reduction of Φ_I was mainly due to the increase of Φ_{NA} in the RPM. Moreover, decrease of the spectral peak value along with blue-shift of the peak position of PSI 77 K fluorescence emission peak were also observed in the seedlings developed in the RPM, suggesting a possible decrease of the amount of PSI proteins and a reduction of energy transfer to PSI core due to increase of the free, uncoupled LHCI (Fig. 4) (Liu et al. 2012; Murata and Satoh 1986).

Furthermore, loss of PSI subunits was observed in the RPM seedlings (Fig. 6), consistent with the reduction of PSI activity. There were 23 and 26 % decrease of subunits of PSI core, PsaA and PsaB, and 11–30 % decrease of Lhca1-4 in the RPM seedlings according to immunoblot analysis, while PsaA/B and two minor subunits of PSI were decreased by 36–64 % according to BN/SDS-PAGE analysis. PSI catalyzes the last step of the light-driven photosynthesis electron transport, the oxidation of the soluble electron carrier plastocyanin and the reduction of ferredoxin, providing energy for carbon dioxide assimilation. In higher plants, PSI consists of at least 15 core subunits (PsaA to PsaL and PsaN to PsaP), four different light harvesting antenna proteins (Lhca1-4), and a large number of cofactors. PsaA and PsaB are strongly-coupled PSI reaction center subunits, formed a heterodimer that binds the primary electron-donor P700 (Dekker and Boekema 2005). The formation of the heterodimeric core PsaA/PsaB initiates the assembly of PSI and provides the scaffold for other subunits of PSI. Reduction of PsaA and PsaB along with other minor subunits of PSI core may lead to loss of PSI accumulation and PSI function under RPM condition (Kouril et al. 2005; Lunde et al. 2000; Redding et al. 1999; Rochaix 1997). Decreases of Lhca1-4 under RPM further reduce the absorption cross section for light harvesting, thus limit the excitation energy transfer to PSI. Lhcas also play a role in the protection of PSI reaction center under high-light, thus decrease of Lhcas may lead to photoinhibition of PSI (Shikanai et al. 1998). Decreases of two Cyt b_6f subunits, Rieske Fe–S protein, and Cyt f, which participated in electron transfer between PSII and PSI, and NdhH, which mediates PSI cyclic electron transport (Alboresi et al. 2009; Peng et al. 2012), also induce negative effect on PSI activity under RPM. Immunoblot analysis also showed a reduction of β-subunit of ATPase under RPM condition. The chloroplast ATP synthase catalyzes the light-driven synthesis of ATP and acts as a key feedback regulatory component of photosynthesis. Decrease of $CF_1\beta$ under RPM may reduce the electron transport of the acceptor side of PSI, corresponding with the decrease of PSI charge separation.

Taken together, our data on fluorescence induction, TL, 77 K fluorescence emission spectra, redox kinetics of P700, and biochemical analyses clearly reveal that PSI is down-regulated under RPM condition, while PSII remains unchanged. PSI is generally believed to be more stable and resistant than PSII under environmental stress conditions (Berry and Björkman 1980; Havaux 1996). However, recent studies suggested that PSI can be more vulnerable in some plant species under specific environmental conditions. For example, photoinhibition of PSI is more conspicuous than PSII in chilling sensitive plants under low temperature stress (Sonoike 2006, 2011). Controversial results were often reported in former spaceflight researches on photosynthesis. Reductions of in vitro PSI electron transport rate and PSI absorption cross-section were observed in spaceflight *B. rapa* (Jiao et al. 2004; Kochubey et al. 2004; Stutte et al. 2005), while no change of PSII activity (Kochubey et al. 2004), or coinstantaneous decline of PSII electron transport rate (Stutte et al. 2005) were reported in their reports. By using RPM to simulate microgravity effects, we managed to control the plant growth environment sufficiently, and make proper ground controls and replicates which cannot be easily achieved under spaceflight conditions. Based on the results in this study, we demonstrate that PSI is more susceptible than PSII under RPM condition. RPM induces degradation of both PSI core and its outer antenna complexes, thus leads to decline of PSI activity. On the other hand, the amounts of PSII proteins and PSII photosynthetic activity are unaffected by the RPM condition. However, clinorotation cannot totally substitute real microgravity, it is of great important to further study the functions of PSI and PSII in future spaceflight researches.

In conclusion, the results present in this study suggest that RPM induces down-regulation of PSI photosynthetic activity and accumulation of PSI proteins, while the function and proteins of PSII remain unchanged. Decrease in the amplitude of absorbance changes of P700 and Φ_I, blue-shift and reduction of 77 K PSI fluorescence emission peak were found in the RPM plants. No distinct destruction was observed in the thylakoid membranes of the RPM

samples. Our results suggested that PSI is more susceptible than PSII under RPM condition.

Acknowledgments This study was supported by the Frontier Project of the Knowledge Innovation Engineering of Chinese Academy of Sciences (KJCX2-YW-L08) and the Chinese manned spaceflight project.

References

Adamchuk NI (1998) Ultrastructural and functional changes of photosynthetic apparatus of *Arabidopsis thaliana* (L.) Heynh. induced by clinorotation. Adv Space Res 21:1131–1134

Adamchuk NI, Guikema JA, Jiao S, Hilaire E (2002) State of *Brassica rapa* photosynthetic membranes in microgravity. J Gravit Physiol 9:229–230

Alboresi A, Ballottari M, Hienerwadel R, Giacometti GM, Morosinotto T (2009) Antenna complexes protect photosystem I from photoinhibition. BMC Plant Biol 9:71

Arnon DI (1949) Copper enzymes in isolated chloroplasts. Polyphenoloxidase in *Beta vulgaris*. Plant Physiol 24:1–15

Barjaktarović Ž, Nordheim A, Lamkemeyer T, Fladerer C, Madlung J, Hampp R (2007) Time-course of changes in amounts of specific proteins upon exposure to hyper-g, 2-D clinorotation, and 3-D random positioning of *Arabidopsis* cell cultures. J Exp Bot 58:4357–4363

Berry J, Björkman O (1980) Photosynthetic response and adaptation to temperature in higher plants. Annu Rev Plant Physiol 31: 491–543

Borst AG, van Loon JJWA (2009) Technology and developments for the random positioning machine, RPM. Microgravity Sci Technol 21:287–292

Bradford MM (1976) A rapid and sensitive method for the quantitation of microgram quantities of protein utilizing the principle of protein-dye binding. Anal Biochem 72:248–254

Buchen B, Hoson T, Kamisaka S, Masuda Y, Sievers A (1993) Development of statocyte polarity under simulated microgravity on a 3-D clinostat. Biol Sci Space 7:111–115

Chen X, Zhang W, Xie Y, Lu W, Zhang R (2007) Comparative proteomics of thylakoid membrane from a chlorophyll *b*-less rice mutant and its wild type. Plant Sci 173:397–407

Dekker JP, Boekema EJ (2005) Supramolecular organization of thylakoid membrane proteins in green plants. Biochim Biophys Acta 1706:12–39

Demeter S, Vass I (1984) Charge accumulation and recombination in photosystem II studied by thermoluminescence. I. Participation of the primary acceptor Q and secondary acceptor B in the generation of thermoluminescence of chloroplasts. Biochim Biophys Acta 764:24–32

Ducruet J-M, Vass I (2009) Thermoluminescence: experimental. Photosynth Res 101:195–204

Dutcher FR, Hess EL, Halstead TW (1994) Progress in plant research in space. Adv Space Res 14:159–171

Eley JH, Myers J (1964) Study of a photosynthetic gas exchanger: a quantitative repetition of the Priestley experiment. Texas J Sci 16:296–333

Govindjee (1995) Sixty-three years since Kautsky: chlorophyll a fluorescence. Aust J Plant Physiol 22:131–160

Havaux M (1996) Short-term responses to photosystem I to heat stress. Photosynth Res 47:85–97

Hoson T, Kamisaka S, Masuda Y, Yamashita M, Buchen B (1997) Evaluation of the three-dimensional clinostat as a simulator of weightlessness. Planta 203:S187–S197

Inoue Y (1996) Photosynthetic thermoluminescence as a simple probe of photosystem II electron transport. In: Amesz J, Hoff J (eds) Biophysical techniques in photosynthesis, series advances in photosynthesis and respiration, vol 3. Kluwer, Dordrecht, pp 93–107

Jiang YD, Li WN, Wang LF, Zhang ZY, Zhang BM, Wu HJ (2008) Space several new type of clinostats. Space Med Med Eng 21:368–371

Jiao S, Hilaire E, Paulsen AQ, Guikema JA (2004) *Brassica rapa* plants adapted to microgravity with reduced photosystem I and its photochemical activity. Physiol Plant 122:281–290

Kitaya Y, Kawai M, Tsuruyama J, Takahashi H, Tani A, Goto E, Saito T, Kiyota M (2001) The effect of gravity on surface temperature and net photosynthetic rate of plant leaves. Adv Space Res 28:659–664

Klughammer C, Schreiber U (1994) An improved method, using saturating light pulses, for the determination of photosystem I quantum yield via $P700^{+}$-absorbance changes at 830 nm. Planta 192:261–268

Klughammer C, Schreiber U (1998) Measuring p700 absorbance changes in the near infrared spectral region with a dual wavelength pulse modulation system. In: Garab G (ed) Photosynthesis: mechanisms and effects, vol V. Kluwer, Dordrecht, pp 4357–4360

Klughammer C, Schreiber U (2008) Saturation pulse method for assessment of energy conversion in PS I. PAM Appl Notes 1:11–14

Kochubey SM, Adamchuk NI, Kordyum EI, Guikema JA (2004) Microgravity affects the photosynthetic apparatus of *Brassica rapa* L. Plant Biosyst 138:1–9

Kordyum EL, Adamchuk NI (1997) Clinorotation affects the state of photosynthetic membranes in *Arabidopsis thaliana* (L.) Heynh. J Gravit Physiol 4:77–78

Kouril R, Zygadlo A, Arteni AA, de Wit CD, Dekker JP, Jensen PE, Scheller HV, Boekema EJ (2005) Structural characterization of a complex of photosystem I and light harvesting complex II of *Arabidopsis thaliana*. Biochemistry 44:10935–10940

Kraft TFB, van Loon JJWA, Kiss JZ (2000) Plastid position in *Arabidopsis* columella cells is similar in microgravity and on a random-positioning machine. Planta 211:415–422

Krause GH, Weis E (1991) Chlorophyll fluorescence and photosynthesis: the basics. Annu Rev Plant Physiol Plant Mol Biol 42:313–349

Krüger GHJ, Tsimilli-Michael M, Strasser RJ (1997) Light stress provokes plastic and elastic modifications in structure and function of photosystem II in camellia leaves. Physiol Plant 101:265–277

Laemmli UK (1970) Cleavage of structural proteins during the assembly of the head of bacteriophage T4. Nature 227:680–685

Liu J, Yang H, Lu Q, Wen X, Chen F, Peng L, Zhang L, Lu C (2012) PSBP-DOMAIN PROTEIN1, a nuclear-encoded thylakoid lumenal protein, is essential for photosystem I assembly in *Arabidopsis*. Plant Cell 24:4992–5006

Long SP, Zhu X-G, Naidu SL, Ort DR (2006) Can improvement in photosynthesis increase crop yields? Plant Cell Environ 29:315–330

Lunde C, Jensen PE, Haldrup A, Knoetzel J, Scheller HV (2000) The PSI-H subunit of photosystem I is essential for state transitions in plant photosynthesis. Nature 408:613–615

Martínez-García JF, Monte E, Quail PH (1999) A simple, rapid and quantitative method for preparing *Arabidopsis* protein extracts for immunoblot analysis. Plant J 20:251–257

Meurer J, Meierhoff K, Westhoff P (1996) Isolation of high-chlorophyll-fluorescence mutants of *Arabidopsis thaliana* and their characterisation by spectroscopy, immunoblotting and Northern hybridization. Planta 198:385–396

Monje O, Stutte G, Chapman D (2005) Microgravity does not alter plant stand gas exchange of wheat at moderate light levels and saturating CO_2 concentration. Planta 222:336–345

Moore R (1990) How effectively does a clinostat mimic the ultrastructural effects of microgravity on plant cells? Ann Bot 65:213–216

Murata N, Satoh K (1986) Absorption and fluorescence emission by intact cells, chloroplasts and chlorophyll–protein complexes. In: Amesz J, Fork DC, Govindjee (eds) Light emission by plants and bacteria. Academic Press, London, pp 137–159

Musgrave ME, Kuang A, Brown CS, Matthews SW (1998) Changes in *Arabidopsis* leaf ultrastructure, chlorophyll and carbohydrate content during spaceflight depend on ventilation. Ann Bot 81:503–512

Myers J (1954) Basic remarks on the use of plants as biological gas exchanges in a closed system. J Aviation Med 25:407–411

Nechitailo GS, Mashinsky AL (1993) Ultrastructure of plant cells during spaceflight. In: Nechitailo GS, Mashinsky AL (eds) Space biology. Mir Publishers, Moscow, pp 331–366

Nedukha EM (1997) Effects of microgravity on the structure and function of plant cell walls. Int Rev Cytol 170:39–77

Parry MAJ, Reynolds M, Salvucci ME, Raines C, Andralojc PJ, Zhu X-G, Price GD, Condon AG, Furbank RT (2011) Raising yield potential of wheat. II. Increasing photosynthetic capacity and efficiency. J Exp Bot 62:453–467

Peng L, Ma J, Chi W, Guo J, Zhu S, Lu Q, Lu C, Zhang L (2006) Low PSII Accumulation1 is involved in efficient assembly of photosystem II in *Arabidopsis thaliana*. Plant Cell 18:955–969

Peng L, Fukao Y, Fujiwara M, Shikanai T (2012) Multistep assemble of chloroplast NADH dehydrogenase-like subcomlpex A requires several nucleus-encoded proteins, including CRR41 and CRR42 in *Arabidopsis*. Plant Cell 24:202–214

Perbal G (2006) Plant Development in Microgravity. In: Clément G, Slenzka K (eds) Fundamentals of space biology, research on cells, animals, and plants in space. Microcosm Press and Springer, New York, pp 227–290

Pfündel E, Klughammer C, Schreiber U (2008) Monitoring the effects of reduced PS II antenna size on quantum yields of photosystems I and II using the Dual-PAM-100 measuring system. PAM Appl Notes 1:21–24

Redding K, Cournac L, Vassiliev IR, Golbeck JH, Peltier G, Rochaix J-D (1999) Photosystem I is indispensable for photoautotrophic growth, CO_2 fixation, and H_2 photoproduction in *Chlamydomonas reinhardtii*. J Biol Chem 274:10466–10473

Rochaix J-D (1997) Chloroplast reverse genetics: new insights into the function of plastid genes. Trends Plant Sci 2:419–425

Rutherford AW, Crofts AR, Inoue Y (1982) Thermoluminescence as a probe of photosystem II photochemistry: the origin of the flash-induced glow peaks. Biochim Biophys Acta 682:457–465

Salisbury FB (1991) Lunar farming: achieving maximum yield for the exploration of space. HortScience 26:827–833

Shikanai T, Endo T, Hashimoto T, Yamada Y, Asada K, Yokota A (1998) Directed disruption of the tobacco *ndhB* gene impairs cyclic electron flow around photosystem I. Proc Natl Acad Sci USA 95:9705–9709

Soh H, Auh C, Soh W-Y, Han K, Kim D, Lee S, Rhee Y (2011) Gene expression changes in *Arabidopsis* seedlings during short to long-term exposure to 3-D clinorotation. Planta 234:255–270

Sonoike K (2006) Photoinhibition and protection of photosystem I. In: Golbeck JH (ed) Photosystem I: the light-driven plastocyanin: ferredoxin oxidoreductase, series advances in photosynthesis and respiration, vol 24. Springer, Dordrecht, pp 657–668

Sonoike K (2011) Photoinhibition of photosystem I. Physiol Plant 142:56–64

Strasser BJ, Strasser RJ (1995) Measuring fast fluorescence transients to address environmental questions: the JIP test. In: Mathis P (ed) Photosynthesis: from light to biosphere, vol 5. Kluwer, Dordrecht, pp 977–980

Strasser RJ, Srivastava A, Govindjee (1995) Polyphasic chlorophyll a fluorescence transients in plants and cyanobacteria. Photochem Photobiol 61:32–42

Stutte GW, Monje O, Goins GD, Tripathy BC (2005) Microgravity effects on thylakoid, single leaf, and whole canopy photosynthesis of dwarf wheat. Planta 223:46–56

Stutte GW, Monje O, Hatfield RD, Paul A-L, Ferl RJ, Simone CG (2006) Microgravity effects on leaf morphology, cell structure, carbon metabolism and mRNA expression of dwarf wheat. Planta 224:1038–1049

Tang Y, Wen X, Lu C (2005) Differential changes in degradation of chlorophyll–protein complexes of photosystem I and photosystem II during flag leaf senescence of rice. Plant Physiol Biochem 43:193–201

Tripathy BC, Brown CS, Levine HG, Krikorian AD (1996) Growth and photosynthetic responses of wheat plants grown in space. Plant Physiol 110:801–806

Vass I, Horváth G, Herczeg T, Demeter S (1981) Photosynthetic energy conservation investigated by thermoluminescence. Activation energies and half-lives of thermoluminescence bands of chloroplasts determined by mathematical resolution of glow curves. Biochim Biophys Acta 634:140–152

Volovik OI, Kordyum EL, Guikema JA (1999) Some characteristics of photosynthetic apparatus under conditions of spaceflight. J Gravit Physiol 6:127–128

Wei N, Tan C, Qi B, Zhang Y, Xu G, Zheng H (2010) Changes in gravitational forces induce the modification of *Arabidopsis thaliana* silique pedicel positioning. J Exp Bot 61:3875–3884

Wheeler RM, Stutte GW, Subbarao GV, Yorio NC (2001) Plant growth and human life support for space travel. In: Passarakli M (ed) Handbook of plant and crop physiology, 2nd edn. Marcel Dekker, New York, pp 925–941

Wolff SA, Coelho LH, Zabrodina M, Brinckmann E, Kittang A-I (2013) Plant mineral nutrition, gas exchange and photosynthesis in space: a review. Adv Space Res 51:465–475

Wolverton C, Kiss JZ (2009) An update on plant space biology. Gravit Space Biol 22:13–20

Zhang Y, Ding S, Lu Q, Yang Z, Wen X, Zhang L, Lu C (2011) Characterization of photosystem II in transgenic tobacco plants with decreased iron superoxide dismutase. Biochim Biophys Acta 1807:391–403